# Statistics of prelocalized states in disordered conductors

Vladimir I. Fal'ko*
*Max-Planck-Institut für Festkörperforschung, Heisenbergstrasse 1, 70569 Stuttgart, Germany and Institute of Solid State Physics RAS, Chernogolovka, 142432 Russia*

K. B. Efetov
*Max-Planck-Institut für Physik Komplexer Systeme, Heisenbergstrasse 1, 70569 Stuttgart, Germany and L.D. Landau Institute for Theoretical Physics, Moscow, Russia*
(Received 12 July 1995)

The distribution function of local amplitudes, $t = |\psi(\mathbf{r}_0)|^2$, of single-particle states in disordered conductors is calculated on the basis of a reduced version of the supersymmetric $\sigma$ model solved using the saddle-point method. Although the distribution of relatively small amplitudes can be approximated by the universal Porter-Thomas formulas known from the random-matrix theory, the asymptotical statistics of large $t$'s is strongly modified by localization effects. In particular, we find a multifractal behavior of eigenstates in two-dimensional (2D) conductors which follows from the noninteger power-law scaling for the inverse participation numbers (IPN's) with the size of the system, $Vt_n \propto L^{-(n-1)d^*(n)}$, where $d^*(n) = 2 - \beta^{-1}n/(4\pi^2\nu D)$ is a function of the index $n$ and disorder. The result is valid for all fundamental symmetry classes (unitary, $\beta_u = 1$; orthogonal, $\beta_o = \frac{1}{2}$; symplectic, $\beta_s = 2$). The multifractality is due to the existence of prelocalized states which are characterized by a power-law form of statistically averaged envelopes of wave functions at the tails, $|\psi_t(r)|^2 \propto r^{-2\mu}$, $\mu = \mu(t) < 1$. The prelocalized states in short quasi-one-dimensional (1D) wires have the tails $|\psi(x)|^2 \propto x^{-2}$, too, although their IPN's indicate no fractal behavior. The distribution function of the largest-amplitude fluctuations of wave functions in 2D and 3D conductors has logarithmically normal asymptotics.

## I. INTRODUCTION

Localization of a particle by a random potential has been extensively investigated during the past several decades.[1–6] It is well known[5–7] that, at strong disorder, single-particle wave functions are confined and have exponentially decaying tails beyond the scale of the localization length $L_c$. At weak disorder, the localization length can be very large in one-dimensional (1D) and 2D conductors, and infinite in 3D. A natural question arises: What is the behavior of the wave functions at distances smaller than the localization length? Despite its importance, the problem of the structure of quantum states of weakly disordered conductors for scales below the length $L_c$ has only recently started to attract interest.[8–17]

In particular, one of the issues that has not been explored up to now concerns the way the localized states develop as a consequence of the increase of disorder in an isolated piece of a metal, though a great deal is already known about the extended states in it. Some part of the recent results related to the extended (metallic-type) states has been obtained by mapping the problem of quantum mechanics in the classically chaotic systems to the Wigner-Dyson random-matrix theory,[18–21] or using the zero-dimensional supermatrix $\sigma$ model,[7,22–26] which are two equivalent ways of describing disordered and chaotic systems.

Both the advantage and disadvantage of such an approach come from the statistical equivalence of eigenstates, which is usually built into the construction of the random matrix substituting the real dynamics. In particular, this reveals the set of universalities of the spectra, the level-level correlations and the transition matrix elements,[19] which are similar for a wide variety of objects. For example, the distribution function of local densities of wave functions $|\psi(\mathbf{r}_0)|^2$ in a chaotic cavity, which one can find in such a way, is determined only by the fundamental symmetry of the system and its volume $V \sim L^d$, but is independent of the level of disorder (i.e., of the value of a mean free path $l$) or a physical dimension, $d$.

On the other hand, this approach hides individual features of physically different systems and permits us to describe *only metallic-type states*, which equally test the random potential all over the sample. More complex states, which can distinguish between the ballistic and diffusive regimes, have to be analyzed beyond the conventional random-matrix theory. Numerical evidence for their existence has been obtained by several groups.[10–12,15] The goal of the theory to be presented in the present paper is to find manifestations of these *precursors of localization* among the wave functions of classically diffusive conductors ($p_F l \gg 1$, $l \ll L$). That is, we consider an isolated piece of a disordered metal with dimensions $l \ll L < L_c$, assuming that the internal "conductance" $g$, which one would assign to the "electric circuit" connecting the observation point (blown up to the mean free path size), with the external surface of the

 

specimen[27] is much larger than the conductance quantum, i.e., $g \gg 1$. In the following sections, we perform a statistical analysis of local densities and partly reconstruct the spatial structure of those rare states, which have locally too high amplitudes (as compared to the average $V^{-1}$) to fit into the universal random-matrix theory description. As can be suggested on the basis of the theory below, these states are responsible for non-Gaussian tails of distributions of fluctuations of local densities of states and conductances suggested by Altshuler, Kravtsov, and Lerner[9] and are generic for the long-living current relaxation discussed in Refs. 9 and 17.

Our paper is organized as follows. In Sec. II, we introduce the notion of the eigenstates statistics (II A), discuss the universal distributions of metallic-type states (II B) and, then, sketch the main results of the paper focusing our attention at the localization effects (II C). Sections III and IV are devoted to the presentation of our theoretical scheme: We derive a reduced supersymmetric $\sigma$ model and show that it has a nontrivial saddle point. The details of the derivation of the saddlepoint solutions of the reduced $\sigma$ model are given separately for each of the fundamental symmetry classes (unitary, orthogonal, and symplectic) in Secs. IV A–IV C, and the influence of fluctuations around the saddle point is discussed in Sec. IV D and the Appendixes. The resulting statistics of wave functions and the structure of the prelocalized states in the conducting regime in quasi-one-dimensional (Q1D), three-dimensional (3D), and in the most interesting case of two-dimensional (2D) samples are discussed in Secs. V, VI, and VII, respectively. Section VIII contains a brief summary of our results and their discussion.

## II. METALLIC VERSUS PRELOCALIZED STATES IN THE EIGENSTATES STATISTICS (PRELIMINARIES AND RESULTS)

In this section, we give a mathematical formulation to the problem of the eigenvalues statistics in disordered systems and consider alternative approaches to its solution. That is what subsection A is about. The next part B is devoted to the universal statistics of metallic type of states known in the random-matrix theory as the Porter-Thomas distribution. The localization effects, which are beyond the random-matrix theory approach, are discussed in subsection C, where we give an essence of the obtained results. This subsection is written for the first reading and can be used as a guide through the rest of the text.

### A. Definitions of the eigenstates statistics

To define the statistics, which we shall be studying in this paper, we first mention that the properly normalized eigenstates $\{\psi_\alpha\}$ that we consider below correspond to a quantum particle in a disordered cavity,

$$\left\{\frac{\mathbf{P}^2}{2M}+U(\mathbf{r})\right\}\psi_\alpha(\mathbf{r})=\epsilon_\alpha\psi_\alpha(\mathbf{r}),\ \psi_\alpha(\mathbf{r}\in S)=0,$$

where $U$ is a random potential. The local amplitude $\psi$ of a wave function at some observation point $\mathbf{r}_0$ inside the sample, i.e.,

$$t\equiv|\psi(\mathbf{r}_0)|^2, \tag{1}$$

will be the object of our statistical analysis. In the meaning of statistical analysis, we employ studies of two related quantities:[28] the distribution function $f(t)$ of local amplitudes $t$ averaged over disorder,

$$f(t)=\Delta\left\langle\sum_\alpha\delta\left[t-|\psi_\alpha(\mathbf{r}_0)|^2\right]\delta(\epsilon-\epsilon_\alpha)\right\rangle, \tag{2}$$

and the set of generalized inverse participation numbers (IPN's) (Refs. 8 and 15), which are the moments of the distribution function $f$,

$$t_n=\Delta\left\langle\sum_\alpha|\psi_\alpha(\mathbf{r}_0)|^{2n}\delta(\epsilon-\epsilon_\alpha)\right\rangle\equiv\int_0^\infty t^n f(t)dt\ . \tag{3}$$

As indicated, $t\langle\ \rangle$ denotes the averaging over random configurations of a random potential $U$ in the system. In Eq. (3), the sum is over the full set of states $\{\psi_\alpha\}$, $V$ is the volume of the system, and $\Delta=(\nu V)^{-1}$ denotes the mean level spacing with $\nu=\nu(\epsilon)$ the density of states per unit volume. Since the distribution function $f$ and wave functions $\{\psi_\alpha\}$ are normalized, one has the following relations:

$$t_0=\int_0^\infty f(t)dt\equiv 1;\ t_1=\left\langle|\psi_\alpha|^2\right\rangle\equiv V^{-1}.$$

One can also introduce the distribution $f_s(\sigma,t)$ of a local spin density of the wave with $\sigma=\downarrow,\uparrow$. It is an important quantity for systems with a strong spin-flip scattering. In random-matrix theory, these systems belong to a symplectic ensemble. Their statistics can be formulated in terms of spin-projected eigenstates, e.g., $t_\downarrow=|\psi_\downarrow(\mathbf{r}_0)|^2$.[29,30] The distribution of a total local density ($t=t_\downarrow+t_\uparrow$) can be found as the convolution,

$$f_s(t)=\int_0^t f(\downarrow,t-t')f(\downarrow,t')dt'. \tag{4}$$

Historically, the studies of eigenstates in disordered conductors started from Wegner's perturbative calculations of IPN's.[8] Due to the equivalence between the descriptions based on the distribution function and the full set of its moments,[28] in most of the later studies[9,22,31] the eigenstates statistics were reconstructed from the set of IPN's. Alternatively, one can start from calculating directly the entire distribution function,[22,32,25,33] especially regarding the possibility to apply the supersymmetry technique.[7] This alternative approach has already been used for describing the eigenstates statistics over the entire crossover regime from the orthogonal to unitary ensembles (low magnetic fields).[25] More recently, this construction has been advanced by developing a reduced $\sigma$ model which is applicable to closed systems.

The reduced $\sigma$ model has nontrivial saddle-point solutions, which enabled us to consider the localization effects nonperturbatively.[33]

The idea of working with the distribution function as a whole also has the additional advantage of making it possible to select those rare states which do not fit to the universal statistics, and to study their spatial structure. The latter information is implicit in the cross-correlation function $R(t,r)$,

$$R(t,r)=\Delta\left\langle\sum_{\alpha}\delta\left[t-|\psi_{\alpha}(\mathbf{r}_0)|^2\right]|\psi_{\alpha}(\mathbf{r}_0+\mathbf{r})|^2\delta(\epsilon-\epsilon_{\alpha})\right\rangle. \tag{5}$$

As will be clear from the calculations below, rare prelocalized states show up as deviations of the function in Eq. (2) from universal distributions at the tails, where $t \gg V^{-1}g$, so that the combination $R(t,r)/f(t)$ mimics the envelope $|\psi_t(r)|^2$ of these states at distances $r=|\mathbf{r}|>l$ from the top-amplitude ($t$) position.

### B. Metallic states and universal statistics

To find the manifestation of prelocalized states in the distribution function $f(t)$, we have, for comparison, to give an idea about what would be the form of the distribution function if all states were extended. Qualitatively, extended states test the realization of a random potential equivalently all over the sample and that is why their statistics coincide with the Porter-Thomas eigenstates statistics renowned in the random-matrix theory.[20,19] Recent studies of properties of eigenstates of disordered and ballistic chaotic cavities [using either the numerical tools[20,21] or the zero-dimensional limit (0D) of the supersymmetric nonlinear $\sigma$ model[7,22,23,26]] have confirmed such an expectation.

Depending on the fundamental symmetry class, the Porter-Thomas distributions can be represented as follows. For the single-particle Hamiltonian describing a spinless particle in the system with a broken (e.g., by a magnetic field) time-reversal symmetry (unitary class), the distribution function of local amplitudes and the corresponding IPN's have the form

$$f_u(t)=V\exp\{-Vt\},\ t_n=n!V^{-n}, \tag{6}$$

whereas in the case of a system with the time-reversal symmetry (orthogonal ensemble),

$$f_o(t)=\sqrt{\frac{V}{2\pi t}}\exp\left\{-\frac{Vt}{2}\right\},\ t_n=\frac{(2n-1)!!}{V^n}. \tag{7}$$

For spin-$\frac{1}{2}$ particles, which undergo a strong spin-orbit interaction (symplectic ensemble), the Porter-Thomas type of a distribution can be repeated both for the spin-projected wave functions and for the total density and has the form

$$f(\downarrow,t)=2Ve^{-2Vt};\ f_s(t)=4V^2te^{-2Vt}\ . \tag{8}$$

### C. Localization effects and eigenstates statistics beyond the universal limit

The universal statistics described by Eqs. (6)–(8) are presented only as a reference point for the subsequent analysis. The rare events, which cannot be described on its basis, have to be studied using more sophisticated methods, and need a treatment of the nonlinear $\sigma$ model beyond 0D limit. Details of these calculation are presented in Secs. IV–VII, whereas in the forthcoming subsection, we sketch only the basic results. In few words, the universal disorder-independent laws work well enough either until this disorder is so weak that the system behaves as in the nearly ballistic regime or at small amplitudes $t<V^{-1}\sqrt{g}$. But they are partly broken or, at least, modified after the disorder makes the electron motion diffusive. In one- and two-dimensional conductors, this requires a different statistical treatment of states which have too high splashes of a local amplitude, $t>V^{-1}\sqrt{g}$.

The method of taking into account all finite (i.e., not only small) inhomogeneous variations of the fields used in the supersymmetric field theory is based on the existence of a saddle point in the nonlinear $\sigma$ model discovered by Muzykantskii and Khmelnitskii.[17] The presence of a saddle point is especially prominent for a reduced version of the $\sigma$ model, which was formulated and solved for the unitary symmetry ensemble in Ref. 33. An interesting result of Ref. 33 for the *quantum diffusion in the dimension* $d=2$ is the *multifractality* of the states, which is in agreement with previous numerical simulations.[11,15] Using the same saddle-point method as for the unitary ($u$) symmetry class,[33] we extend the analysis of 2D systems to the ensembles of other fundamental symmetries (orthogonal, $o$; symplectic, $s$; spin unitary,[34] $su$) and arrive, again, at the multifractality. The latter is manifested by the following scaling of INP's:

$$Vt_n\propto L^{-(n-1)d^*},\ d^*(n)=2-\frac{\beta^{-1}n}{4\pi^2\nu D}\ ,$$
$$\beta_u=1,\ \beta_o=\frac{1}{2},\ \beta_{s,su}=2\ . \tag{9}$$

The fractal, or generalized Rényi dimensions, $d^*(n)$, obey Eq. (9) only for those $n$'s where they are positive and are obtained in the leading order in $(2\pi\nu D)^{-1}$, where $D$ is the classical diffusion coefficient. The sensitivity of the derived statistics to boundary conditions, as well as the form of the correlation function $R(t,r)$, which we find in our calculations, enable us to suggest such a behavior of 2D multifractal states, which is associated with the power-law behavior of statistically averaged envelopes of their tails, $|\psi(\mathbf{r}_0+\mathbf{r})|^2\propto(l/r)^{2\mu}$. Being extended from the position of a rare high-amplitude splash $|\psi(\mathbf{r}_0)|^2=t\gg1$, these tails have exponents $\mu(t)$ individual for each state marked by its own $t$.

The behavior of *prelocalized states in a Q1D wire* within the localization length scale $L_c$ also resembles the power-law localization. Independently of $t$, $|\psi(x_0+x)|^2\propto L_cx^{-2}$. The density of wave functions accumulated by these tails is integrable, so that no assertion about fractality can be made, and the inverse participation numbers

$t_n$ tend to take a volume-independent form for $n > g$.

The *localization effects in 3D conductors* are weak, if disorder is weak enough to keep the system far away from the metal-insulator transition, $p_F l \gg 1$. As a result, the statistics of eigenstates in a 3D conductor is most similar to the universal one: Amplitude $t$ scales with $V$, and the mean free path $l$ appears only as an extra parameter both in the distribution function $f = f(Vt, p_F l)$, and inverse participation numbers $t_n \propto V^{-n}\kappa(n, p_F l)$.

Nevertheless, even then the statistics of rare events show strong deviations from the Porter-Thomas formulas. We obtain for both 2D and 3D diffusive samples the *logarithmically normal distribution* of large local amplitudes of wave functions,

$$f(t) \approx \exp\left\{-\beta\frac{\pi^2\nu D}{\eta_d}\ln^2 T\right\}, \quad T = \frac{Vt\eta_d}{2\pi^2\nu D}, \tag{10}$$

where $\eta_2 = \ln\frac{L}{l}$ and $\eta_3 \sim (2l)^{-1}$. Although we study an isolated specimen, this result strikingly resembles the asymptotics of distributions of local density of states or conductance fluctuations found in open systems.[9] This signals deep physical reasons behind it related, probably, to the properties of random walk paths.

## III. EIGENSTATES PROBLEM IN TERMS OF A NONLINEAR SUPERSYMMETRIC $\sigma$ MODEL

In the following paragraphs, we formulate the eigenstates statistics problem in terms of the nonlinear $\sigma$ model. The details of this technique are described in a review article,[7] and below we give only a compressed extraction from it, keeping similar notations.

One can try to use the supersymmetry technique as soon as a physical quantity of interest is expressed in terms of retarded and advanced Green's functions,

$$G_\epsilon^{R,A}(\mathbf{r},\mathbf{r}) = \sum_\alpha \frac{|\psi_\alpha(\mathbf{r})|^2}{\epsilon - \epsilon_\alpha \pm i\gamma/2}. \tag{11}$$

In Eq. (11), $\gamma$ is level broadening. In an isolated sample, one has to take the limit of $\gamma \to 0$. Due to the discreteness of the spectrum of levels $\{\epsilon_\alpha\}$, this extracts only $\epsilon_\alpha$, the closest to the current energy slice $\epsilon$. Using the expression in Eq. (11) and taking the limit of $\gamma \to 0$, one can formalize the statistics of Eq. (2) in such a way that[25]

$$f(t) = \Delta \lim_{\gamma\to 0}\left\langle \int \frac{d\mathbf{r}'}{2\pi i}\left[G_\epsilon^A(\mathbf{r}',\mathbf{r}') - G_\epsilon^R(\mathbf{r}',\mathbf{r}')\right] \times\delta\left[t - i\gamma V G_\epsilon^R(\mathbf{r},\mathbf{r})\right]\right\rangle. \tag{12}$$

The reformulation of Eq. (12) in terms of the $\sigma$ model exploits the fact[22] that any product of Green functions,

$$i^{n+1}\left[G_\epsilon^R(\mathbf{r},\mathbf{r})\right]^n G_\epsilon^A(\mathbf{r}',\mathbf{r}') \tag{13}$$

$$= \frac{-1}{n!}\int |s_1(\mathbf{r}')|^2 |s_2(\mathbf{r})|^{2n} e^{-L(\Psi)} D\Psi,$$

can be represented as a functional integral over the eight-component supervector field $\Psi = (\Psi_1, \Psi_2)$, $\Psi_m = \frac{1}{\sqrt{2}}(\chi_m^*, \chi_m, s_m^*, s_m)$. The supervector $\Psi$ is composed of four anticommuting and four commuting variables $\chi$ and $s$, respectively. The indices $m = 1, 2$ appear in order to distinguish between advanced and retarded Green functions. Besides $\Psi$, the charge-conjugate field $\bar{\Psi}$ should be defined; one can find this definition in Ref. 7. The action $L(\Psi)$,

$$L(\Psi) = i\int \bar{\Psi}(\mathbf{r})\left[\epsilon - \hat{H}_0 - U(\mathbf{r}) - i\frac{\gamma}{2}\Lambda\right]\Psi(\mathbf{r})d\mathbf{r}, \tag{14}$$

$$\Lambda^{11} = -\Lambda^{22} = \hat{1}\,,$$

incorporates both the free-particle Hamiltonian $\hat{H}_0$ and the random impurity potential $U(\mathbf{r})$.

After Gaussian averaging over $U$,[7] we derive a new Lagrangian with an interaction of the superfields $\Psi$. The interaction term can be decoupled by the functional integration over a supermatrix field $Q$, so that any calculation is finally reduced to the evaluation of a functional integral,

$$\int DQ \exp\{-F[Q]\}W(Q), \tag{15}$$

over slow-varying superfields $Q(\mathbf{r})$. This manipulation is analogous to the introduction of an effective order parameter in the theory of superconductivity. The free energy, which determines weights of different configurations of $Q$, appears after integrating over fast modes and has the form

$$F[Q] = \int d\mathbf{r}\left[-\frac{1}{2}\mathrm{Str}\ln\left(-i\hat{H}_0 + \frac{\gamma}{2}\Lambda + \frac{Q}{2\tau}\right) + \frac{\pi\nu}{8\tau}\mathrm{Str}Q^2\right]. \tag{16}$$

The "anomalous mean" $Q$ can be found from the self-consistency condition,

$$\pi\nu Q = \int dp\left(-i\hat{H}_0 + \gamma\Lambda/2 + Q/2\tau\right)^{-1}, \tag{17}$$

which minimizes $F[Q]$.

In the limit of $\gamma \to 0$, the solutions of Eq. (17) take the values

$$Q = V\Lambda\bar{V}, \quad \bar{V}V = 1\,, \tag{18}$$

from the degeneracy space of one of the graded symmetry groups.[35] This field-theoretical model is strongly nonlinear, since the matrix $Q$ satisfies the condition $Q^2 = 1$, and operations of the conjugation $V \to \bar{V}$ and the supertrace (Str) in Eq. (16) are those defined in Ref. 7. The

"rotation" $V$,

$$V=\begin{pmatrix} u_1 & 0 \\ 0 & v_1 \end{pmatrix} \exp\begin{pmatrix} 0 & -iu_2\dfrac{\hat{\theta}}{2}\bar{v}_2 \\ -iv_2\dfrac{\hat{\theta}}{2}\bar{u}_2 & 0 \end{pmatrix}, \quad (19)$$

is parametrized with the equal number of commuting and anticommuting variables. The second matrix in the product in Eq. (19) is composed only of commuting ones. All anticommuting variables are collected into the matrices $u_1$ and $v_1$. Smooth spatial variations of the $Q$ field at the length scale longer than the mean free path $l$ and the influence of a small but finite value of $\gamma$ can be taken into account by the effective free energy functional,

$$F[Q]=\frac{\pi\nu}{4}\int d\mathbf{r}\mathrm{Str}\left[\frac{D}{2}(\nabla Q)^2-\gamma\Lambda Q\right]. \quad (20)$$

The extension of this equation to the case of spin-$\frac{1}{2}$ particles can be found in Ref. 7, too.

To transform the formulas in Eqs. (2)–(5) into integrals over the $Q$ space, we expand the $\delta$ function in Eq. (12) into the formal series in $G^R_\epsilon$, and study the averages

$$\left\langle i^{n+1}\left[G^R_\epsilon(\mathbf{r},\mathbf{r})\right]^n\int d\mathbf{r}' G^A_\epsilon(\mathbf{r}',\mathbf{r}')\right\rangle$$

for all $n$'s. Using Eq. (13), each of them can be represented as a functional integral over the field $\Psi$ and then modified into the construction

$$\lim_{\mu,\lambda\to 0}\int\frac{d\zeta_1 d\zeta_2}{(2\pi)^2}\frac{(-1)^n n!}{2(2n)!}\partial_\mu\partial^n_\lambda\left\langle\int D\Psi e^{-L(\Psi)-\delta L(\Psi)}\right\rangle.$$

In the latter equation, we perform an additional integration over the phases $\zeta_{1,2}$ [which are hidden into the vectors $\bar{v}_1=\sqrt{2}(0,0,e^{i\zeta_1},e^{-i\zeta_1},0,0,0,0)$, $\bar{v}_2=\sqrt{2}(0,0,0,0,0,0,e^{i\zeta_2},e^{-i\zeta_2})$] and add to the Lagrangian from Eq. (14) a weak perturbation $\delta L$,

$$\delta L=\int d\mathbf{r}'\left[\mu(\bar{v}_1\Psi(\mathbf{r}'))(\bar{\Psi}(\mathbf{r}')v_1)+\lambda(\bar{v}_2\Psi(\mathbf{r}'))(\bar{\Psi}(\mathbf{r}')v_2)\delta(\mathbf{r}'-\mathbf{r})\right].$$

After this, we have to evaluate the generating functional $\langle\int D\Psi e^{-L(\Psi)-\delta L(\Psi)}\rangle$. Its exponent differs from that in Eqs. (15)–(20) only by the perturbation,

$$\delta\hat{H}=i\int d\mathbf{r}'\left[\mu v_1\otimes\bar{v}_1+\lambda v_2\otimes\bar{v}_2\delta(\mathbf{r}'-\mathbf{r})\right],$$

added to the Hamiltonian $\hat{H}_0$ in Eq. (16). The latter results in an additional term $\delta F$ in the free energy functional; we find $\delta F$ by expanding the logarithmical expression in Eq. (16) into the series in $\mu$ and $\lambda$. Doing that, we keep only the contributions up to the first order in $\mu$, whereas "cross terms" which originate from pairing of $\Psi$'s at different coordinates ($\mathbf{r}$ and $\mathbf{r}'$) can be neglected. As an intermediate step, we obtain

$$\delta F=\frac{\mu}{2}\pi\nu(\bar{v}_1 Q v_1)+\frac{1}{2}\ln\left[1+\lambda\pi\nu(\bar{v}_2 Q v_2)\right],$$

and after some algebra, we arrive at

$$f(t)=\int\frac{d\zeta}{2\pi}\lim_{\gamma\to 0}\int DQ\left[\int\frac{d\mathbf{r}}{4V}\mathrm{Str}(\pi_1 Q(\mathbf{r}))\right]\times\delta\left(t-\frac{\pi\nu\gamma}{2}\mathrm{Str}(\Upsilon(\zeta)Q(\mathbf{r}_0))\right)e^{-F[Q]}, \quad (21)$$

where

$$\pi_1=\begin{pmatrix}\pi_b & 0\\ 0 & 0\end{pmatrix},\ \pi_2=\begin{pmatrix}0 & 0\\ 0 & \pi_b\end{pmatrix},\ \pi_b=\begin{pmatrix}0 & 0\\ 0 & 1\end{pmatrix}\otimes\tau_0,$$

and

$$\Upsilon(\zeta)=\pi_2 e^{i\zeta\tau_3}(\tau_0+\tau_1)e^{-i\zeta\tau_3}.$$

Everywhere below, $\tau_i$ are the Pauli matrices, and $\tau_0$ is a $2\times 2$ unit matrix.

## IV. REDUCED $\sigma$ MODEL AND ITS SOLUTION USING SADDLE-POINT METHOD

Based on Eq. (21), we can obtain the full statistics of local amplitudes $|\psi|^2$ for any regime. As we mentioned before, the universal expressions of Eqs. (6)–(8) can be rederived by assuming the zero-dimensional (0D) limit: the coordinate-dependent field $Q(\mathbf{r})$ has to be replaced by its value at the observation point, $Q(\mathbf{r}_0)\equiv Q_0$, which transforms the functional integral in Eq. (21) into a definite integral over $Q_0$.

To go beyond the 0D approximation, one should take into account inhomogeneous fluctuations of the field $Q$. If we integrate over $Q_0=V_0\Lambda\bar{V}_0$, any functions in Eqs. (2)–(4) can be finally expressed in terms of relative rotations of the $Q$ field, with respect to its value at $\mathbf{r}_0$. This is the *reduced $\sigma$ model*. For its derivation, it is significant to note that the degeneracy space of the supermatrix $Q$ is noncompact. Due to this property, the main contribution to the integral in Eq. (21) comes from the region of large $Q_0$'s where $\mathrm{Str}(\Upsilon Q_0)\propto 1/\gamma$. As a result, finite variations of $Q(\mathbf{r})$ produced by means of local rotations $Q(\mathbf{r})\to Q(\mathbf{r}')=V(\mathbf{r},\mathbf{r}')Q(\mathbf{r})\bar{V}(\mathbf{r},\mathbf{r}')$ of the supermatrix field along the noncompact "direction" can be taken into account consistently, since they cover only relatively small environs of an "infinitely large" $Q_0$.

Using the decomposition $V(\mathbf{r})=V_0\tilde{V}(\mathbf{r})$, we define supermatrices $\tilde{Q}$ of the reduced $\sigma$ model as

$$\tilde{Q}=\tilde{V}\Lambda\tilde{\bar{V}},\quad Q(\mathbf{r})=V_0\tilde{Q}(\mathbf{r})\bar{V}_0,\quad \tilde{Q}(\mathbf{r}_0)=\Lambda. \quad (22)$$

Due to the invariance of the $Q$ space, the transformation of Eq. (22) preserves the form of the gradient term in the free energy $F$ in Eq. (20), whereas the second term in $F$ can be modified as

$$F_2=-\frac{\pi\nu\gamma}{4}\int d\mathbf{r}\mathrm{Str}(\tilde{Q}_0\tilde{Q}(\mathbf{r})),\quad \tilde{Q}_0=\bar{V}_0\Lambda V_0.$$

A corresponding substitution can be done in the preexponential in Eq. (21), too. The explicit form and exact parametrization of the matrix $Q_0$ varies from one sym-

metry ensemble to another. Nonetheless, in the limit of $\gamma \to 0$, those parameters of the $Q$ space, which are responsible for its noncompactness, appear in the argument of the $\delta$ function in Eq. (21) in the same combination with the factor $\gamma$ that enters to the "potential" part of the free energy, $F_2$. Therefore, integrating over $Q_0$ in this limit, we eliminate $\gamma$ and convert Eq. (21) into expressions that relate the distribution function $f(t)$ to the generating functionals represented in terms of the fields $\tilde{Q}$. Recently, Muzykantskii and Khmelnitskii[17] have generated an idea that the supersymmetric $\sigma$-model formulation of the localization theory can be treated using the saddle-point method. As will be clearly seen from the form of the effective action incorporated to the generating functionals of the reduced $\sigma$ model, the latter has a nontrivial saddle point, which will be the central object of studies in following subsections.

The parametrization of $Q$ matrices, and, therefore, the derivation and form of the reduced $\sigma$ model depend on the fundamental symmetry of the system. In parts A, B, and C of this section, we specify this for unitary, orthogonal, and symplectic symmetry classes separately, though it turns out that the most essential part of our calculation—the use of the solution of the saddle-point equation described in subsection D—is quite similar for all of them.

### A. Unitary ensemble

In the unitary case, the parametrization of the $Q$ field using Eq. (19) includes "angles"

$$\hat{\theta} = \begin{pmatrix} \theta\tau_0 & 0 \\ 0 & i\theta_1\tau_0 \end{pmatrix}, \quad 0 < \theta < \pi, \quad 0 < \theta_1 < \infty ,$$

where only one of them is imaginary and makes the symmetry group noncompact. Matrices $u_2$ and $v_2$ in Eq. (19), are diagonal and can be trivially eliminated from Eq. (21) as well as the external phases $\zeta$. Other details of the integration over $Q_0$ are the same as those in Ref. 25.

The distribution function $f$,

$$f_u(t) = \frac{1}{V}\frac{d^2\Phi_u(t)}{dt^2}, \tag{23}$$

and the inverse participation numbers $t_n$, $n \geq 2$,

$$t_n \equiv \int_0^\infty t^n f(t)dt = \frac{n(n-1)}{V}\int_0^\infty t^{n-2}\Phi_u(t)dt, \tag{24}$$

can be related to the generating functional $\Phi_u(t)$ of the reduced $\sigma$ model,

$$\Phi_u(t) = \int_{\tilde{Q}(\mathbf{r}_0)=\Lambda} D\tilde{Q}(\mathbf{r})e^{-F_u[t,\tilde{Q}]}. \tag{25}$$

The free energy $F_u$ in Eq. (25) has the form

$$F_u[t,\tilde{Q}] = \int d\mathbf{r}\mathrm{Str}\left[\frac{\pi\nu D}{8}(\nabla\tilde{Q})^2 - \frac{t}{4}\Lambda\Pi\tilde{Q}(\mathbf{r})\right], \tag{26}$$

and we remind you that $\tilde{Q}(\mathbf{r}_0) = \Lambda$ at the origin. The projection operator $\Pi$ in Eq. (26) is defined as

$$\Pi = \begin{pmatrix} \pi_b & \pi_b \\ \pi_b & \pi_b \end{pmatrix}, \ \pi_b = \begin{pmatrix} 0 & 0 \\ 0 & \tau_0 \end{pmatrix}, \tag{27}$$

and selects from the $Q$ matrix only its noncompact sector.

The generating functional $\Phi_u(t)$ has several funny features. First, at $t = 0$, it has a completely invariant form, and, therefore, is equal to unity, which corresponds to the normalization of the wave functions,

$$Vt_1 = \Phi_u(0) \equiv 1. \tag{28}$$

On the other hand, for any finite $t$, the reduced $\sigma$ model is a model with a broken symmetry, so that the free energy in Eq. (26) can be minimized by an inhomogeneous solution $\tilde{Q}(\mathbf{r})$. Indeed, $\frac{t}{4}\Lambda\Pi$ in the second term in Eq. (26) looks like a field tending to align the matrix $\tilde{Q}$ along the noncompact "direction" of the $Q$ space (related to the parameter $\theta_1$), whereas the boundary condition at $\mathbf{r}_0$ together with the gradient term is a rigidity attempting to prevent that. The competition between these two tendencies results in an optimal configuration of $\tilde{Q}$. To find such an optimal configuration (saddle point), we use, again, the invariance of the $Q$ space with respect to rotations $\tilde{V}$ and represent $Q$ as

$$\tilde{Q}(\mathbf{r}) = V_t(\mathbf{r})\Lambda\frac{1+iP}{1-iP}\bar{V}_t(\mathbf{r}), \ P = \begin{pmatrix} 0 & B \\ \bar{B} & 0 \end{pmatrix}, \tag{29}$$

where a weak perturbation $P$ stands for fluctuations around the saddle point, and the matrices $B, \bar{B}$ can be decomposed into blocks as follows:

$$B = \begin{pmatrix} s_{1,1}\tau_0 + is_{1,2}\tau_3 & \hat{\sigma}_1 \\ \hat{\sigma}_2^+ & s_{2,1}\tau_0 + is_{2,2}\tau_3 \end{pmatrix}, \tag{30}$$

$$\hat{\sigma}_\alpha = \begin{pmatrix} \sigma_\alpha & 0 \\ 0 & -\sigma_\alpha^* \end{pmatrix}.$$

The form of the saddle point, $\tilde{Q}_t = V_t\Lambda\bar{V}_t$, follows from the requirement of the absence of linear terms in the expansion $F_u$ into the series,

$$F_u[t,\tilde{Q}] = F_t + F^{(2)} + F^{(3)} + F^{(4)} + \dots , \tag{31}$$

in the perturbation $P$. This selects

$$V_t = \exp\begin{pmatrix} 0 & \frac{1}{2}\theta_t e^{i\chi\tau_3} \\ \frac{1}{2}\theta_t e^{-i\chi\tau_3} & 0 \end{pmatrix}, \tag{32}$$

where the parameter $\theta_t(\mathbf{r})$ satisfies the optimum equation,

$$\Delta\theta_t(\mathbf{r}) = -\frac{t}{\pi\nu D}e^{-\theta_t}; \ \chi = \pi, \tag{33}$$

with the boundary conditions $\theta_t(\mathbf{r}_0) = 0$ in the origin and $(\mathbf{n}\nabla)\theta_t = 0$ at the surface of a sample. In Eq. (33), $\Delta$ stands for the Laplacian in the real space. This equa-

tion is partly similar to the saddle-point equation derived by Muzykantskii and Khmelnitskii[17] when studying the problem of long-living current relaxation in open conductors, but it has a different nonlinearity and different boundary conditions.

As will be clear from the following analysis, a general solution of the saddle-point equation requires the possibility of considering singular confugurations of $e^{-\theta}$ in dimensions $d = 2$ and 3. The treatment of singularities can be done in two ways: using an equivalent formulation of the field theoretical problem on the lattice with the site about the mean free path,[36] or cutting off short distances and replacing the boundary conditions in a single point by conditions at the surface with the radius about the mean free path $l$. In the following, we choose the second way.

### B. Orthogonal ensemble

The parametrization of $Q$ matrices in the orthogonal ensemble is more complicated due to a larger number of independent parameters in it. In particular, the noncompact sector of the degeneracy space is parametrized by two "imaginary angles"—variables $\theta_{1,2}$:

$$\hat{\theta} = \begin{pmatrix} \theta\tau_0 & 0 \\ 0 & i(\theta_1\tau_0 + \theta_2\tau_1) \end{pmatrix}, \quad \begin{matrix} 0 < \theta < \pi, \\ 0 < \theta_{1,2} < \infty. \end{matrix}$$

Unitary matrices $u_2$ and $v_2$ in Eq. (19) have a more complicated form, too,

$$u_2 = \begin{pmatrix} M & 0 \\ 0 & e^{i\phi\tau_3} \end{pmatrix}, \; v_2 = \begin{pmatrix} \tau_0 & 0 \\ 0 & e^{i\chi\tau_3} \end{pmatrix},$$

$$M = \frac{1 - i\vec{m}\vec{\tau}}{1 + i\vec{m}\vec{\tau}},$$

where $0 \le \phi, \chi < 2\pi$, $m_{1,2,3}$ are real, and the number of anticommuting variables in $u_1$ and $v_1$ is twice as large as in the unitary case.

The integration over $Q_0$ can be performed in a complete analogy with the unitary-symmetry case, but with several distinguishing features. First of all, in the limit of $\gamma \to 0$, the main contribution comes from the region of the $(\theta_1, \theta_2)$ plane, where $\cosh\theta_1 \cosh\theta_2 \sim 1/\gamma$. Since the product $\cosh\theta_1 \cosh\theta_2$ can be large at large $\theta_1$ as well as at large $\theta_2$, we end up with a different form of projection operators,

$$\Pi_o = \begin{pmatrix} \pi_b(o) & \pi_b(o) \\ \pi_b(o) & \pi_b(o) \end{pmatrix}, \; \pi_b(o) = \begin{pmatrix} 0 & 0 \\ 0 & \tau_0 + \tau_1 \end{pmatrix},$$

in the free energy,

$$F_o[t', \tilde{Q}] = \int d\mathbf{r} \mathrm{Str} \left[ \frac{\pi\nu D}{8} (\nabla\tilde{Q})^2 - \frac{t'}{8} \Lambda\Pi_o \tilde{Q}(\mathbf{r}) \right]. \quad (34)$$

This $\Pi_o$ determines the direction of an effective "force" along the symmetrically chosen noncompact "direction" $(\theta_1 + \theta_2)$.

Next, in the orthogonal ensemble, one has to keep the external phase factor $e^{i\xi}$ in Eq. (21) until the end of the integration over $Q_0$, which results in the integrodifferential relation,

$$f_o(t) = \frac{4}{V\pi\sqrt{t}} \frac{d^2}{dt^2} \left\{ \int_0^\infty dz \Phi_0(t + z^2) \right\}, \quad (35)$$

between the distribution function $f_o$ and generating functional,

$$\Phi_o(t') = \int_{\tilde{Q}(\mathbf{r}_0)=\Lambda} D\tilde{Q} \exp(-F_o[t', \tilde{Q}]) . \quad (36)$$

The generating functional $\Phi_o(t')$ gives directly the inverse participation numbers $t_n$, $n \ge 2$,

$$t_n = \frac{2}{\sqrt{\pi}V} \frac{\Gamma(n + 1/2)}{\Gamma(n - 1)} \int_0^\infty (t')^{n-2} \Phi_o(t') dt', \quad (37)$$

and, again, has the property $\Phi_o(0) = Vt_1 \equiv 1$.

To study the fluctuations near the saddle point, we represent $\tilde{Q}$ in the form of Eq. (29), where

$$B = \frac{B_+ + B_-}{\sqrt{2}},$$

$$B_\pm = \begin{pmatrix} (s_{11}^\pm \tau_0 + i s_{12}^\pm \tau_3)\tau_\pm & \hat{\sigma}_1^{(\pm)} \\ (\hat{\sigma}_2^{(\pm)})^+ & (s_{21}^\pm \tau_0 + i s_{22}^\pm \tau_3)\tau_\pm \end{pmatrix},$$

and

$$\hat{\sigma}_\alpha^{(\pm)} = \begin{pmatrix} \sigma_\alpha^\pm & \pm\sigma_\alpha^\pm \\ \mp(\sigma_\alpha^\pm)^* & -(\sigma_\alpha^\pm)^* \end{pmatrix}, \; \tau_\pm = \tau_0 \pm \tau_1 .$$

In this decomposition, $s_{\alpha\beta}^\pm$ are real numbers, $\sigma_\alpha^\pm$ and $(\sigma_\alpha^\pm)^*$ —anticommuting variables. Indices "±" are introduced for later convenience. Everywhere below, we keep superscript "−" but omit "+."

Similarly to the unitary case, the free energy $F_o$, which governs the generating functional $\Phi_o$, has the minimum at $\tilde{Q} = V_t \Lambda \bar{V}_t$,

$$V_t = \exp \begin{pmatrix} 0 & e^{i\chi\tau_3} \sum_\pm \frac{\theta_t^\pm \tau_\pm}{4} e^{-i\phi\tau_3} \\ e^{i\phi\tau_3} \sum_\pm \frac{\theta_t^\pm \tau_\pm}{4} e^{-i\chi\tau_3} & 0 \end{pmatrix}$$

where the variables $\theta_t \equiv \theta_1 + \theta_2$, $\theta_t^- \equiv \theta_1 - \theta_2$ and $\chi, \phi$ satisfy the following equations:

$$\Delta\theta_t(\mathbf{r}) = -\frac{t'}{\pi\nu D}e^{-\theta_t},\ \Delta\theta_t^-(\mathbf{r}) = 0,\ e^{i(\chi\pm\phi)} = -1\ . \quad (38)$$

The conditions at the origin and boundary are the same as in the unitary case. The latter gives $\theta_t^-(\mathbf{r}) = 0$, and the nontrivial saddle point is related only to the symmetric variable $\theta_t$.

### C. Symplectic ensemble

An analogous investigation of the statistics of spin-polarized electron waves in the case of a strong spin-flip scattering needs an extension of dimensions of $Q$ matrices and the following analysis of the degeneracy space related to their gapless Goldstone modes. The gaps in the spectrum of $Q$'s appear due to a large spin-relaxation rate, $\tau_s^{-1}$, which can be caused both by the spin-orbit coupling built into the material properties or by the spin-flip scattering on a classical randomly oriented static magnetic field. In the former case, the time-reversal symmetry is conserved, whereas in the latter this invariance is violated by the source of a scattering. Since triplet components of $Q$ correspond to gapfull modes,[5,7] only singlet modes have to be taken into account, so that the number of independent variables of $Q$ is the same as in the spinless case. One has to remember only that all matrix elements of $Q$ are multiplied by the unit $2 \times 2$ spin matrix $\tilde{\tau}_0$.

In this subsection, we work with the distribution $f(\downarrow, t)$ of a local spin density $t \equiv |\psi_\downarrow|^2$ of eigenstates, which we defined by Eq. (5) and above. To incorporate spins into Eq. (21), one can substitute

$$\pi_{1,2} \to \pi_{1,2} \otimes \tilde{\tau}_0,\ \Upsilon \to \Upsilon \otimes \tilde{\tau}_\downarrow,$$

where "$\otimes$" stands for the direct product of matrices, and $\tilde{\tau}_i$ are spin operators: $\tilde{\tau}_0 = \begin{pmatrix} 1 & 0 \\ 0 & 1 \end{pmatrix}$, $\tilde{\tau}_\downarrow = \begin{pmatrix} 0 & 0 \\ 0 & 1 \end{pmatrix}$.

The degeneracy space of $Q_0$ is noncompact along a single direction, and the integration over $Q_0$ gives us

$$f(\downarrow, t) = \frac{1}{2V}\frac{d^2\Phi_s(t)}{dt^2},\quad \Phi_s(t) = \int D\tilde{Q}(\mathbf{r})e^{-F_s[t,\tilde{Q}]}\ , \quad (39)$$

where

$$F_s[t,\tilde{Q}] = \int d\mathbf{r}\mathrm{Str}\left[\frac{\pi\nu D}{4}(\nabla\tilde{Q})^2 - \frac{t}{2}\Lambda\Pi\tilde{Q}(\mathbf{r})\right]\ , \quad (40)$$

and $\Pi$ is exactly the same as in Eq. (27).

From the point of view of the rest of calculations, the case with a broken time-reversal invariance is equivalent to the spinless unitary-symmetry class.[7] That is why we mark the quantities related to this symmetry with a label "$su$" and generate the distribution function $f_{su}(\downarrow, t)$ from the distribution function $f_u(t)$ in Eqs. (23)–(26) as

$$f_{su}(\downarrow, t) = 2f_u(2t) \text{ at } D \to 2D\ .$$

Concerning the symplectic ensemble with the time-reversal symmetry, it demands an extra calculation, since in the presence of spin-orbit interactions it cannot be reduced to the spinless orthogonal one. The parametrization of the $Q$ space in this case is given by Eq. (19) with

$$\hat{\theta} = \begin{pmatrix} \theta\tau_0 + \theta'\tau_1 & 0 \\ 0 & i\theta_1\tau_0 \end{pmatrix},\ 0 < \theta, \theta' < \pi,\ 0 < \theta_1 < \infty,$$

and

$$u_2 = \begin{pmatrix} e^{i\phi\tau_3} & 0 \\ 0 & M \end{pmatrix},\ v_2 = \begin{pmatrix} e^{i\chi\tau_3} & 0 \\ 0 & \tau_0 \end{pmatrix}\ ,$$

$$M = \frac{1 - i\vec{m}\vec{\tau}}{1 + i\vec{m}\vec{\tau}}\ ,$$

where $0 \le \phi, \chi < 2\pi$, and $m_{1,2,3}$ are real variables. After this, the saddle-point configuration of $\tilde{Q}$ for the symplectic case can be found as $\tilde{Q}_t = V_t\Lambda\bar{V}_t$,

$$V_t = \exp\begin{pmatrix} 0 & \frac{\theta_t}{2}M \\ \frac{\theta_t}{2}M^+ & 0 \end{pmatrix}\ ,$$

where $\theta_t$ satisfies the optimum equation and the matrix $M$ is chosen in such a way that $M = -\tau_0$:

$$\Delta\theta_t(\mathbf{r}) = -\frac{t}{\pi\nu D}e^{-\theta_t},\ |m| \to \infty, \quad (41)$$

with the boundary conditions $\theta_t(\mathbf{r}_0) = 0$ in the observation point and $(\mathbf{n}\nabla)\theta_t = 0$ at the surface.

### D. Optimal free energy and fluctuations near the saddle point

After comparing the saddle-point equations in Eqs. (33),(38),(41), one finds that they are similar in different symmetry classes. The difference between the unitary, orthogonal, and symplectic ensembles leads only to different values of a coefficient $\beta$,

$$\beta_o = \frac{1}{2},\ \beta_u = 1,\ \beta_{su} = \beta_s = 2\ , \quad (42)$$

in the expression for the optimal free energy,

$$F_t = \beta\int d\mathbf{r}\left\{\frac{\pi\nu D}{2}(\nabla\theta_t)^2 + te^{-\theta_t}\right\}\ , \quad (43)$$

and in the higher-order terms of the expansion of $F[t,\tilde{Q}]$ in the environs of the saddle point. The generating functional $\Phi(t)$ from Eqs. (25),(36),(39) can be represented in the form

$$\Phi(t) = J(t)\exp(-F_t).$$

In the conducting regime, the value of the optimal free

energy determines the leading term in the exponential of the generating functional, whereas the effect of fluctuations around the saddle point is included into the function $J(t)$,

$$J(t) = \int DP \exp\{-F^{(2)} - F^{(3)} - F^{(4)} \cdots\} . \quad (44)$$

Due to the normalization condition in Eq. (28), the relation $J(0) = 1$ holds exactly, and the contribution from the fluctuations $P$ can be calculated by expanding the exponential in the integrand in Eq. (44) into the series in the higher-order terms $F^{(3,4,\ldots)}$ and performing Gaussian integrations over $P$ with the weight $\exp\{-F^{(2)}\}$ determined by the second-order correction to the free energy.

The applicability of such a perturbation theory is justified by the fact that the higher orders are, at least, by the factor of $(2\pi\nu D)^{-1} \ll 1$ smaller, as compared to what is given by

$$J(t) \approx \int DP \exp\{-F^{(2)}[t, P]\} . \quad (45)$$

The latter is nothing but the superdeterminant of the Hamiltonian related to the fluctuations around the saddle point. The value of $J(t)$ differs from unity, merely because the symmetry between fermionic and bosonic degrees of freedom is broken by the optimal solution. Since not all the projections of the infinitesimal $P$ to the generators of the Lie algebra of the graded symmetry group are equivalently affected by the symmetry breaking, it is convenient to separate in $F^{(2)}$ the terms that are affected by the existence of the optimal solution from those that are not. Depending on the physical symmetry class, this involves different sets of variables. Nevertheless, after an appropriate diagonalization, quadratic form $F^{(2)}$ can be represented uniquely for all symmetry classes:

$$F^{(2)} = F_t^{(2)} + \varsigma F_0^{(2)}, \ \varsigma_{u,su} = 0, \ \varsigma_{o,s} = 1 . \quad (46)$$

The term $F_0^{(2)}$ in Eq. (46) is composed of fields, which are not affected by the symmetry breaking,

$$F_0^{(2)} = 2\pi\nu D \sum_{\alpha=1,2} \int d\mathbf{r} \left\{ \vec{\partial}\sigma_\alpha^- \vec{\partial}(\sigma_\alpha^-)^* + \vec{\partial} s_\alpha^- \vec{\partial}(s_\alpha^-)^* \right\} .$$

This term does not contribute to the function $J$ in the Gaussian approximation, due to the symmetry between boson and fermion degrees of freedom incorporated in it. On the contrary, the first term in Eq. (46) is the sum over those four pairs of dynamical variables, which are affected by the violation of the boson-fermion symmetry,

$$F_t^{(2)} = 2\pi\nu D \int d\mathbf{r} \Big\{ \sum_{\alpha=1,2} [\partial\sigma_\alpha \partial\sigma_\alpha^* + U_\sigma \sigma_\alpha \sigma_\alpha^*] + \sum_{\beta,\alpha=1,2} [(\partial s_{\alpha,\beta})^2 + U_s^{\alpha\beta} s_{\alpha,\beta}^2] \Big\} .$$

Due to that, the preexponential $J$ can be represented as

$$J = \exp\left\{ \frac{1}{2} \sum_n \ln \left[ (\chi_\sigma(n))^4 \Big/ \prod_{\alpha,\beta} \chi_s^{\alpha\beta}(n) \right] \right\} , \quad (47)$$

where the sum is extended over all the eigenvalues of the spectral problem,

$$[-\Delta + U - \chi]\phi = 0, \quad \phi(\mathbf{r}_0) = 0, \ \mathbf{n}\nabla\phi(S) = 0. \quad (48)$$

As we already mentioned above, in the quadratic approximation, any difference in $J$ from unity is due to the broken symmetry between fermionic and bosonic degrees of freedom in $P$. The broken symmetry shows up in the Hamiltonian $F_t^{(2)}$ as the difference between the effective potentials,

$$\begin{aligned} U_\sigma &= \tfrac{1}{4}(\nabla\theta_t)^2 + \frac{t}{2\pi\nu D} e^{-\theta_t}, \\ U_s^{\alpha\beta} &= \frac{k_{\alpha,\beta}}{4}(\nabla\theta_t)^2 + \frac{t q_{\alpha,\beta}}{2\pi\nu D} e^{-\theta_t}. \end{aligned} \quad (49)$$

In Eq. (49), $k_{\alpha,1} = q_{\alpha,1} = 0$ and $k_{1,2} = 4$, $k_{2,2} = 0$, $q_{\alpha,2} = 2$. The spectra $\{\chi_\sigma(n)\}$ and $\{\chi_s^{\alpha\beta}(n)\}$ of modes remain gapfull, since all $U > 0$. Moreover, due to the sum rule,

$$\sum_{\alpha\beta} U_s^{\alpha\beta} = 4 \sum U_\sigma , \quad (50)$$

their main contribution to $J$ comes from low-lying eigenvalues of Eq. (48). Since the set of $U$'s in Eq. (49) depends on the form of the saddle point alone, the calculation of the correction to the exponent in this order in $(2\pi\nu D)^{-1}$ can be performed simultaneously for all symmetry classes and is small.

On the other hand, the effect of fluctuations can become important, once we want to extend the consideration of samples with the size larger than the localization length. Such a step, which is beyond of the scope of this paper, would need some kind of a renormalization of the saddle point. We would only like to stress that this could be a way to avoid difficulties in obtaining a stable fixed point in the renormalization group treatment of the localization problem pointed out by several authors.[37–39]

The existence of the saddle point and relatively small contribution from fluctuations in the metallic regime makes it easy to find the form of the cross-correlation function $R(t, r)$ from Eq. (5), too. If we study the envelope (statistically averaged) of the wave function at large enough distances $r \gg l$, from the position of a high-amplitude splash, the reasoning used above can be repeated for $R(t, r)$, with minor modifications, and we arrive at

$$R(t, r)/f(t) \propto t e^{-\theta_t(r)} , \quad (51)$$

so that one can say that the statistical envelope $|\psi_t(r)|^2$ follows the form of the optimal configuration of the reduced $\sigma$ model.

Up until now, we performed our analysis without referring to any specific dimensionality of the system. On the other hand, from Eqs. (33),(38),(41),(48), one can see

that the form of the saddle point and, therefore, the optimal free energy $F_t$ crucially depend on the dimensionality. In the next sections, we discuss the statistics of local amplitudes of wave functions in quasi-one-dimensional, three-dimensional, and two-dimensional conductors separately.

## V. NEARLY LOCALIZED STATES IN A SHORT DISORDERED WIRE

It is well known that the localization effects are the strongest in one-dimensional and Q1D conductors.[2,5] Even when disorder is weak, the quantum diffusion of a particle is blocked at the length scale $L_c = \beta 2\pi\nu D$, where $D$ is the classical diffusion coefficient determined by the elastic impurity scattering[7] and $\beta$ is specified by Eq. (42). In Q1D wires the effective density of states $\nu$ is the local one integrated over cross-sectional width $w$ or an area, $S \sim w^2$, and, therefore, the localization length $L_c \sim l(w/\lambda_F)^{d-1}$ can be much longer than the mean free path $l$. This allows us to consider the short wires $L < L_c$, with an already developed diffusive regime, and below we analyze the distribution of amplitudes and the shape of untypical states, which are the precursors of localization at larger distances. Note, that in the Q1D case, we define the variable $t$ as the wave function density integrated over the cross-sectional area (width) of a wire. Since there is a lot known about the Q1D systems,[2,40,31] it is useful to compare the results of the saddle-point approximation, with the exact calculation based on the transfer-matrix method.[41] From this point of view, the saddle point gives nothing but a "semiclassical" solution of the effective Schrödinger equation in the $Q$ space,[7] which appears in the transfer-matrix method. Such a "semiclassics" not only gives the results, which are very close to the exact solutions,[31] but also enables us to make a statement about the form of statistical envelopes of prelocalized states in the metallic regime.

In the following paragraphs, we apply the scheme of calculus described in the previous section. First of all, we have to solve the saddle-point equation,

$$\partial_x^2 \theta_t(x) = -\frac{t}{\pi\nu D}\exp\{-\theta_t\} , \tag{52}$$

and use its solution $\theta_t(x)$ when calculating the optimal free energy $F_t$. Due to the condition $\theta_t(x_0) = 0$ at the observation point $x_0$, the latter splits the wire with length $L$ into two, not necessarily equal intervals $0 < x < L_{i=L,R}$. The form of $\theta_t(x)$ can be found separately in each of them. In dimension one, the differential equation in Eq. (52) can be solved exactly,[42] and we represent its general solution in the form

$$e^{-\theta_t} = \left[\frac{A_i}{\cos\left\{A_i\sqrt{T_i}\left(1-\frac{x}{L_i}\right)\right\}}\right]^2 , \quad x > 0;\ i = L, R . \tag{53}$$

Although one can notice that the general form of this solution formally contains a singularity at $x_\infty = -L_i[\pi/(2A_i\sqrt{T_i}) - 1]$, the latter is illusory, since it takes place in the nonphysical region $x < 0$ and plays no role unless it comes up to the formulation of the limitations to our theory. The requirement $x_\infty \gg l$, which emerges from the existence of the singular point, is related to the conditions on maximal values of gradients permitted by the use of only the lowest-order gradient expansion terms in the free energy functional in Eq. (21). We shall discuss the consequences of this condition at the end of the section, assuming for a while that it is satisfied. If so, the consistency equations on the parameters $A_i$ come from the boundary conditions $\partial_x\theta_t(L_i) = 0$ at the edges and have the form

$$A_i = \cos\left(A_i\sqrt{T_i}\right) , \tag{54}$$

where $T_i$ are defined as

$$T_i = \frac{tL_i^2}{2\pi\nu D} . \tag{55}$$

The optimal value of the free energy can be found, in its turn, as

$$F_t = \beta\sum_{i=L,R}\frac{L_i t}{\sqrt{T_i}}\left[2\sqrt{1-A_i^2} - A_i^2\sqrt{T_i}\right] . \tag{56}$$

In general, the exact form of $F_t$ in Eq. (56) based on the closed set of Eqs. (53)–(55) can be studied numerically at any values of the parameters included, as illustrated in Fig. 1. On the other hand, a somewhat simpler analytical expression can be written in the asymptotical regions. First of all, we examine the limit of small amplitudes, $T_i < 1$, where the exact distribution has to match the random-matrix theory results. At $T_i < 1$, the results

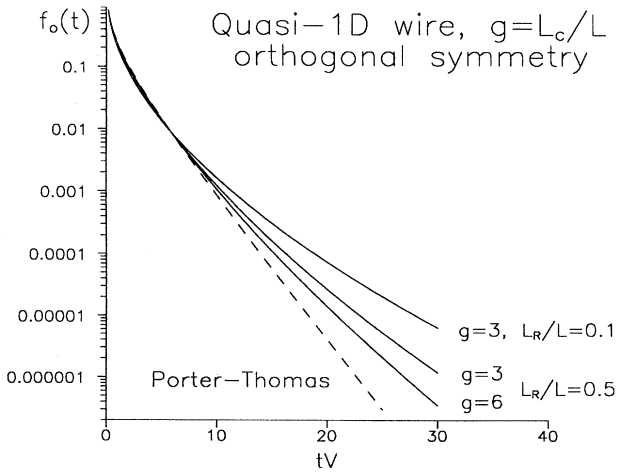


FIG. 1. Distribution function of local amplitudes in Q1D system calculated for the orthogonal symmetry class. Dashed line shows the Porter-Thomas statistics, and solid lines correspond to various levels of disorder and different positions of an observation point inside a sample.

of Eqs. (54)–(56) can be expanded into the series in $T_i$, which gives $A_i \approx 1 - \frac{1}{2}T_i + \frac{13}{24}T_i^2 + \cdots$ and

$$F_t \approx Vt\left(1 - \sum_{i=L,R} \frac{T_i L_i}{3L} + \cdots\right) , \quad f^{(1)}(t) \approx Ve^{-\beta F_t} .$$

We see that in this limit, the Porter-Thomas formulas, Eqs. (6)–(8) give a good approximation for the body of the distribution function $f(t)$, which describes those amplitudes $t$ which are $t < L^{-1}\sqrt{L_c/L}$. Otherwise, the second term of this expansion, $VtT_i$, becomes larger than unity and strongly affects the probability to detect a too high splash of the wave function.

When $T_i \gg 1$, the optimal configuration $e^{-\theta_t}$ develops at the length scale of $\lambda = \sqrt{2\pi\nu D/t}$, where it can be approximated as

$$e^{-\theta_t(x)} \sim (\lambda/x)^2 , \tag{57}$$

and gets less sensitive to the presence of boundaries. Indeed, in the limit of $T_i \gg 1$, one has $A_i \approx \frac{\pi}{2}T_i^{-1/2}(1 - T_i^{-1/2} + \cdots)$, and the exact expression for the optimal free energy can be expanded into the series in $T_i^{-1/2}$,

$$F_t = 4\sqrt{\beta L_c t}\,\{1 - \delta_L - \delta_R\} , \tag{58}$$

where

$$\delta_i \sim \frac{\pi^2}{8}\left[T_i^{-1/2} - \frac{1}{2}T_i^{-1} + \cdots\right], \quad i = L, R .$$

The leading term in Eq. (58) does not depend on the system length and (in the orthogonal ensemble) coincides with the asymptotical behavior of the distribution function of local amplitudes in infinite wires. The latter has been found by Mirlin and Fyodorov[31] on the basis of the analysis of the transfer-matrix equations derived by Efetov and Larkin.[40] Although we did our calculations for the short-length samples, $L < L_c = \beta 2\pi\nu D$, the results for the high-amplitude splashes surprisingly agree with those for the infinite geometry, even up to the leading term in the preexponential factor $J$, which is derived in Appendix A. Roughly speaking, the "semiclassical" solution of the transfer-matrix equation gives an almost exact result. The full form of the tails of $f(t)$ at $t > g/L$, where $g = L_c/L$, can be represented as

$$f^{(1)}(t) \approx C\frac{\sqrt{L_L L_R}}{L}\sqrt{\frac{L_c}{t}}\exp\left[-4\sqrt{\beta L_c t}\,\{1 - \delta_L - \delta_R\}\right], \tag{59}$$

and is applicable up to the amplitudes $t \sim L_c/l^2 \sim w/(l\lambda_F)$. The latter condition emerges from the requirement of a smoothness of the saddle-point solution, so that its characteristic length scale $\lambda = \sqrt{2\pi\nu D/t}$, should be longer than the mean free path, $\lambda > l$. Otherwise, the singularity of the equation in Eq. (53) comes too close to the physical part of the space ($x > 0$), which would create too large gradients forbidden within the used approximation.

The distribution function given by Eq. (59) evidences that the states, which are responsible for the rare event that we discussed in the previous paragraph, are (at least, partly) localized. Nevertheless, even for the largest amplitudes $t > L_c/L^2$, the effect of edges is still present, which means that this in not an exponential localization. On the basis of an analysis of the cross-correlation function $R(t, r)$ from Eqs. (5) and (51), we can say that, within the range of distances $x < L_c$, the *statistical envelope of the density of prelocalized states*, $|\psi_t(x)|^2$ resembles the form of the optimal solution and has the power-law intermediate asymptotics,

$$|\psi_t(x)|^2 \propto te^{-\theta_t} \sim L_c/x^2 . \tag{60}$$

In contrast to the 2D case, which we discuss in Sec. VII, the derived form of a typical wave function has the same exponent for all prelocalized states, independently of the amplitude of their top splashes. Further, the tails of the envelope in Eq. (60) are integrable, so that the inverse participation numbers, which one can find on the basis of Eqs. (3) and (24),(37), do not indicate any fractal behavior.

## VI. EIGENSTATES STATISTICS IN $D = 3$

The localization effects in weakly disordered 3D conductors are known to be the least pronounced,[5] so that their eigenstates statistics have to be most similar to the universal one. Nevertheless, even in this case, not all states are described by the Porter-Thomas distribution, and this section is devoted to the disorder-dependent corrections to formulas in Eqs. (6)–(8) in dimension three.

To describe the statistics beyond the universality limit, we have to solve optimum equations (33),(38),(41). For the sake of simplicity, we consider a spherically shaped conducting particle and place the observation point into its center. This enables us to seek the solutions $\theta_t(r)$ in a symmetric form. Nonetheless, even that does not help us to find the exact form[42] of a general solution of the nonlinear equation,

$$\Delta\theta_t(r) = [r^{-2}\partial_r r^2 \partial_r]\theta_t = -\frac{t}{\pi\nu D}e^{-\theta_t} , \tag{61}$$

so that we have to develop the following approximate procedure. The nonlinear $\sigma$ model, Eq. (20), was derived under the conjecture of smoothly varying $Q$ fields. This implies that the distances shorter than the mean free path $l$ are excluded from our consideration, and the condition $\theta_t(0) = 0$ at the origin has to be substituted by the condition $\theta_t(r_0) = 0$ at the sphere of a radius $r_0 \sim l$. Of course, this is an approximate procedure. If one starts from the equivalent lattice model of the $Q$-field theory,[7] the necessity to deal with the cutoff of singularities vanishes, but it is replaced by an uncertainty in the choice of a basic lattice.[36] In the 2D case the lattice form factor enters under the logarithm, i.e., it plays a minor role. In the 3D case, the form factor enters as a multiplier, which produces an uncertainty up to the numerical coefficient in front of the part of the free energy coming

from short distances, although we believe that functional dependences take a correct form.

After this, we scale the distances by $l$, so that $\theta_t = \theta_t(r/l)$, and solve the problem iteratively. The iterative procedure appeals to the fact that the Laplace equation, which one can get by neglecting the right-hand side of Eq. (61), has nonzero solutions and that the parameter

$$\rho = \sqrt{\pi\nu D/(l^2 t)}$$

which appears after rescaling the distances $r$ with the mean free path is large. The latter condition restricts our consideration to the amplitudes $t < (l\lambda_F^2)^{-1}$, which are smaller than the density formed by the forward-and-backward scattered trajectory between two impurities.

As the first step, we expand the desired function $\theta_t(r)$ as

$$\theta_t \approx \theta_t^{(0)} + \theta_t^{(1)}, \quad \theta_t^{(0)} = A(1 - l/r).$$

The first term in it satisfies the Laplace equation, but does not satisfy the necessary boundary condition at $r = L$. The term $\theta_t^{(1)}$ is added in order to meet the requirement $\partial_r \theta_t = 0$ at the external edge. It must turn to zero at $r = l$ and can be found from the linearized equation,

$$[u^{-2}\partial_u u^2 \partial_u]\theta_t^{(1)} = -\rho^{-2}\exp(-\theta_t^{(0)}), \quad \theta_t^{(1)}(1) = 0,$$

where $u = r/l$. After this, the nonlinearity of Eq. (61) transforms into a self-consistent determination of the parameter $A$, from the algebraic equation,

$$A = \rho^{-2}\int_1^{L/l} u^2 du \exp\{-A(1-u^{-1})\} \approx \frac{1}{3\rho^2}\left(\frac{L}{l}\right)^3 e^{-A},$$

which arises from the requirement $\partial_u \theta_t^{(1)}(L/l) = 0$. One could continue the iterative scheme even further and add corrections, which improve the function $\theta_t^{(1)}(x)$ itself, and so on, but this is not necessary for evaluating the leading terms of the optimal free energy $F_t$. So, we stop the iteration after the first step and find that

$$e^{-\theta_t(r)} = \exp\left[-A(1 - l/r)\right], \; r > l \; . \tag{62}$$

The combination of the parameters, which stands in the right-hand side of Eq. (61) and the self-consistency equation itself, can be rewritten in the form

$$Ae^A = T \equiv \frac{Vt\eta_3}{2\pi^2\nu D} \sim Vt/(p_F l)^2 \; , \tag{63}$$

where $\eta_3 \sim (2l)^{-1}$ and the condition $p_F l \gg 1$ corresponds to the limit of a weak disorder. The optimal free energy related to the saddle-point configuration can be calculated, too, and has the form

$$F_t \approx \beta 2\pi^2 \frac{\nu D}{\eta_3} A\left\{1 + \frac{A}{2}\right\}. \tag{64}$$

When $T \ll 1$, the calculation both of the self-consistent $A$ and the related value of $F_t$ can be performed as an expansion into a series in the parameter $T$, i.e., we approximate $A \approx T - T^2 + \cdots$ and

$$F_t = \beta V t\left[1 - \frac{Vt\eta_3}{4\pi^2\nu D} + \cdots\right] \; , \quad \eta_3 \sim (2l)^{-1} \; .$$

When $T \gg 1$, the leading terms arise from the estimation $A \sim \ln T$. In each of these two regimes, the generating functional $\Phi(t)$ has the form

$$\Phi^{(3)} \approx \begin{cases} \exp\left(-\beta Vt + \beta\dfrac{(Vt)^2\eta_3}{4\pi^2\nu D} + \cdots\right), & T < 1, \\ \exp\left\{-\beta\pi^2\dfrac{\nu D}{\eta_3}\ln^2 T + \cdots\right\}, & T > 1, \end{cases} \tag{65}$$

which can be used for evaluating both the distribution function $f(t)$ and IPN's, using Eqs. (23),(35),(39) and (24),(37). At this point, we have to mention that the coefficient $\eta_3 \sim (2l)^{-1}$ cannot be determined better than by the order of magnitude. We also remind you that different symmetry classes are distinguished by the parameter $\beta$: $\beta_u = 1$, $\beta_o = \frac{1}{2}$, $\beta_s = 2$.

Equation (65) indicates that the noticeable deviations from the universal Porter-Thomas distribution start rising at local densities $tV \sim p_F l$ [the second term in the exponent in Eq. (65) becomes larger than unity] and then develop into the logarithmically normal asymptotics at $tV > (p_F l)^2$. On one hand, the states, which generate such an asymptotical tail, are not typically metallic. On the other hand, both the form of the envelope,

$$|\psi_t(r)|^2 \propto \exp\{-A(1 - l/r)\} \; , \tag{66}$$

which we extract from the shape of the optimal solution in Eq. (62) and the scaling of IPN's with the integer power of the system volume for any $n$,

$$t_n \approx \frac{\min\{\varphi(n), [2\pi^2\nu D/\eta_3]^n\}}{V^n}\exp\left(\frac{n^2\eta_3}{\beta 4\pi^2\nu D}\right),$$

$$\varphi_u = n!, \; \varphi_o = (2n-1)!!, \; \varphi_s = n!/2^n,$$

indicate that these 3D states are not localized in a conventional sense: They always have a finite part of the density in remote parts of a sample. Of course, these extended density tails decrease when $t$ approaches the limiting value $t \sim (l\lambda_F^2)^{-1}$, but our methods do not allow us to make a statement about the structure of standing waves at the scale of $r < l$.

The version of the $\sigma$ model that we used above also restricts our consideration to the metallic regime $p_F l \gg 1$. The development of a theory at critical conditions, $p_F l \leq 1$, requires the use of more sophisticated methods.[43] Nevertheless, the common belief, which arises from most of the known localization theories,[5] is that the dimension $d = 2$ is critical, so that the analysis of wave function statistics in 2D disordered conductors would manifest the important features of the criticality.

## VII. MULTIFRACTALITY OF EIGENSTATES IN WEAKLY DISORDERED 2D CONDUCTORS

To find an optimal configuration in the 2D case, we limit the length scale of the $Q$-field variations from below by the value of a mean free path—similar to what we discussed in the previous section. This modifies the boundary conditions into $\theta_t(r_0) = 0$ at $r_0 \sim l$. For the sake of simplicity, we consider the sample in the form of a disk (with the radius $L$) and place the observation point $\mathbf{r}_0$ right in its center. Then, we seek an axially symmetric solution $\theta_t(r)$ of the equation,

$$(r^{-1}\partial_r r\partial_r)\theta_t = -\frac{t}{\pi\nu D}e^{-\theta_t}.$$

This can be done both exactly[42] or using an iterative procedure developed in Sec. VI.

### A. Exact solution

The exact solution can be represented in the form

$$e^{-\theta_t} = \left[\frac{2(l/r)^{1-A}\left[\sqrt{(\frac{1}{A\rho})^2+1}+1\right]}{\left[\sqrt{(\frac{1}{A\rho})^2+1}+1\right]^2-(\frac{1}{A\rho})^2(\frac{r}{l})^{2A}}\right]^2, \quad (67)$$

where $\rho = \sqrt{\frac{2\pi\nu D}{tl^2}}$, and $A$ has to be found from the boundary condition at the sample edge $r = L$,

$$\sqrt{A^2+\rho^{-2}} + A = \frac{(L/l)^A}{\rho}\sqrt{\frac{1+A}{1-A}}. \quad (68)$$

After substituting $\theta_t(r)$ from Eq. (67) to Eq. (43), we also find the optimal free energy,

$$F_t = \beta 4\pi^2\nu D\left\{\ln\left(\frac{(L/l)^{(1+A^2)}}{\rho^2[1-A^2]}\right) + 2(1-\sqrt{A^2+\rho^{-2}})\right\}.$$

Together with Eq. (68), the latter expression can be studied numerically. The numerical analysis shows that the consistency equation in Eq. (68) has positive roots only if $\rho > \ln(L/l) \gg 1$, which provides a reasonable limitation to the wave functions amplitudes that we can study using this method: We have to restrict the density $t$ of a splash by the value $(\lambda_F l)^{-1}$ related to the density of an electron state bound to the forward-and-backward scattered trajectory between two impurities. At the same time, in the limit of $\rho \gg 1$, the roots of Eq. (68) can be approximated by $A = 1-\mu$, where $\mu < 1$. The same condition gives us the possibility of replacing the exact solution in Eq. (67) by

$$e^{-\theta_t} \approx (l/r)^{2\mu}, \quad (69)$$

which means that there is an easier way to get a satisfactory approximate solution of the saddle-point equation in $d = 2$, similar to what we did in $d = 3$.

### B. Solution using iterations

The result of Eq. (69) can also be derived using the iterative scheme discussed in Sec. VI. Being approved by the strong inequality $\rho \gg 1$, we use, first, the linear Laplace equation by choosing its solution in the form that satisfies the boundary conditions at the origin,

$$\theta_t^{(0)} = 2\mu\ln(r/l),$$

where the parameter $\mu$ will be the subject of the next iteration. That is, we seek $\theta_t = \theta_t^{(0)} + \theta_t^{(1)}(r/l)$, which satisfies the boundary condition at the external edge, and where

$$[u^{-1}\partial_u u\partial_u]\theta_t^{(1)} = -2\rho^{-2}u^{-2\mu},$$
$$\theta_t^{(1)}(1) = 0,\ u = r/l.$$

This gives $\theta_t^{(1)}$ in the form

$$\theta_t^{(1)}(u) = \frac{\rho^{-2}}{2(1-\mu)^2}\left(1-u^{2(1-\mu)}\right).$$

The requirement $\partial_r\theta_t(L) = 0$ gives rise to the consistency equation and enables us to formulate the approximate procedure in the closed form,

$$2\mu = \frac{(L/l)^{2-2\mu}}{(1-\mu)\rho^2}.$$

The use of the iterative procedure is formally limited by a requirement $\theta_t^{(1)} \ll 1$.

The parameter $\mu$ in the above equation can be found [with the accuracy controlled by $1/\ln(L/l) \ll 1$] as

$$\mu = \frac{z(T)}{2\ln(L/l)},\ ze^z = T \equiv \frac{tV\ln(L/l)}{2\pi^2\nu D}, \quad (70)$$

and varies when the amplitude $t$ changes. For example, the crossover of the optimal solution to the homogeneous $\tilde{Q} \equiv \Lambda$ occurs in the limit of $T \ll 1$, where one can find that

$$\mu = \frac{1}{2}T(1-T+\cdots)/\ln\frac{L}{l}.$$

In the opposite limit of large amplitudes, $T \gg 1$,

$$\mu \approx \frac{1}{2}\ln T/\ln\frac{L}{l} < 1.$$

The approximate form of the optimal free energy can be found, in its turn, as

$$F_t \approx \beta 4\pi^2\nu D\left\{\mu + \mu^2\ln\frac{L}{l}\right\}. \quad (71)$$

When $T \ll 1$, this can be expanded in $T$ as

$$F_t \approx \beta V t\left\{1-\frac{T}{2}+\cdots\right\} .$$

When $T \gg 1$ [but still $t \ll (l\lambda_F)^{-1}$], the leading term in the optimal $F_t$ takes the form

$$F_t \approx \beta\pi^2\nu D\frac{\ln^2 T}{\ln(L/l)} .$$

Although the size of the system enters these formulas, the logarithmically weak dependence of $F_t$ on $L$ makes it meaningful to use the derived expressions for an arbitrary position of the observation point inside the sample of an arbitrary convex shape.

The fluctuations around the saddle-point configuration and the resulting preexponential factor $J(t)$ for the 2D case are discussed in Appendix B. All over the conduction regime their contribution is not important, as compared to that of the saddle point itself.

### C. Distribution function and IPN's

All of this enables us to calculate the distribution function $f$ with the exponential accuracy. Figure 2 shows its behavior (for different levels of disorder) in the transient regime, where the deviations from the universal statistics start to develop. Here, we illustrate the behavior of the orthogonal symmetry ensemble, since it corresponds to the experimentally studied case of statistics of the distribution of microwave irradiation in a disordered slab.[44] The numerically calculated $f(t)$ shown in Fig. 2 describes the statistics in the transient regime of not very large amplitudes $t$, whereas the limits of small and large $t$ allow an asymptotical analysis.

For small amplitudes $t < 2\pi\nu D/[L^2 \ln \frac{L}{l}]$, one obtains

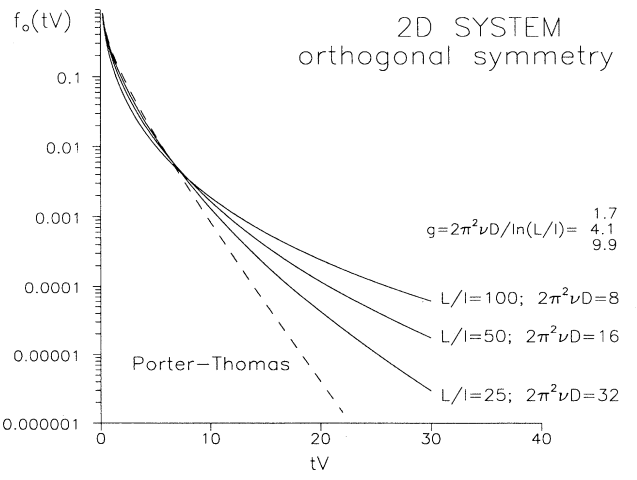


FIG. 2. Distribution function of local amplitudes in a disordered 2D system calculated for the orthogonal symmetry class. Dashed line shows the Porter-Thomas statistics, and solid lines correspond to various levels of disorder.

$$f^{(2)} \approx V\exp\left(-\beta V t\left[1-\frac{T}{2}+\cdots\right]\right)\times\begin{cases}\sqrt{\dfrac{1}{2\pi t V}}, & o\\ 1, & u\\ 2, & s;su\end{cases} , \tag{72}$$

where $T$ is defined in Eq. (70), and

$$\beta_o = \frac{1}{2};\ \beta_u = 1;\ \beta_{s,su} = 2 .$$

In the opposite limit, $t > 2\pi\nu D/[L^2 \ln \frac{L}{l}]$, the distribution function takes the form

$$f^{(2)} \sim V\exp\left(-\frac{\beta\pi^2\nu D}{\ln(L/l)}\ln^2 T\right) . \tag{73}$$

Equations (72) and (73) generalize our earlier result[33] to various symmetry classes. They show that for any of the fundamental symmetries—orthogonal, symplectic, and unitary—disorder makes the appearance of high-amplitude splashes of wave functions much more probable than one would expect from the Porter-Thomas formula and, as concerns the most extraordinary events, tends for the tails to take the logarithmically normal form. When being written for the orthogonal ensemble, the logarithmically normal law in Eq. (65) strikingly coincides with the form of the asymptotics of the distribution of fluctuations of the local density of states and conductances in open systems found in Ref. 9, although our theory was made for closed systems and is based on a different scheme of calculations. This agreement reveals the deep relationship of these two results obviously caused by the localization effects.

But the localization of wave functions, which are responsible for the asymptotic events, is not the localization of a particle in a confining potential in the conventional sense. The tails of these states do not decay exponentially: Even in the asymptotical regime $T \gg 1$, the size $L$ of the system influences the distribution. The splashes look as if they were formed by focusing the waves by some rare configurations of scatterers. In some sense, they are analogous to the scars in the wave functions of chaotic ballistic billiards,[45] though their appearance is of a stochastic origin. The structure of these states can be anticipated from the way the distribution function is affected by the boundary or—directly—from the cross-correlation functions $R(t,r)$ in Eqs. (5),(51). Following the form of the saddle-point configuration, the statistically averaged envelope of the density of such a state has a power-law asymptotic tail,

$$|\psi_t(\mathbf{r})|^2 \sim e^{-\theta_t(r)} \approx (l/r)^{2\mu} , \tag{74}$$

where $\mu < 1$ and tends to approach the limiting value $\mu = 1$ for the highest amplitudes $t \sim (l\lambda_F)^{-1}$.

Moreover, the form of IPN's, $t_n$ derived on the basis of Eqs. (24),(37) shows such a scaling with the size of a system, which implies that they are a multifractal structure. To find the moments $t_n$ accurately enough, we have to take into account that, although the crossover to the 0D case looks like the formal limit $T(t) \to 0$, the Porter-

Thomas statistics fail unless the condition $tV \ll \sqrt{2\pi\nu D}$ is satisfied [see Eq. (72)]. Hence, only the first few ratios $t_n$, $2 \leq n \ll \sqrt{2\pi\nu D}$, can be estimated using a finite polynomial expansion of $f(t)$ into the series in $T$, and their first terms reproduce corrections to the universal statistics found pertubatively in Ref. 26. Alternatively, we derive the higher-order IPN's from Eqs. (3),(24),(36) using the saddle-point method of integration over $t$. The moments $t_n$ calculated in both ways are in good agreement with each other and, in the leading order, can be represented as

$$t_n \approx \frac{\min\{\varphi(n), [2\pi\nu D/\ln\frac{L}{l^\delta}]^n\}}{l^\delta V}\left(\frac{1}{V}\right)^{(n-1)d^*/2}, \quad (75)$$

where

$$d^*(n) \approx 2 - \frac{\beta^{-1}n}{4\pi^2\nu D} \text{ and } \delta = (n-1)(2-d^*). \quad (76)$$

As one can see from Eqs. (75),(76), we end up with such a volume dependence of the inverse participation numbers $t_n$ that manifests the multifractal behavior of quantum states, Eq. (9). The multifractality seems to be the generic property of 2D disordered systems. The multifractal dimensions in Eq. (76) are calculated up to the main order in the inverse conductivity, so that all over the metallic regime, the dependence of $d^*$ on $n$ and disorder is accurate enough and qualitatively agrees with numerical results.[11] Due to the limitation $t < (l\lambda_F)^{-1}$, the above equations work at $n \leq 2\pi\nu D$, so that $n-\delta > 0$, and the fractal dimensions $d^*$ in Eq. (76) are positive.

## VIII. DISCUSSIONS

Summarizing the results of the paper, we studied the manifestation of precursors of localization among the eigenstates of isolated disordered conductors with the size smaller than the localization length. In order to detect these states, we analyzed the statistics of local amplitudes of wave functions, $t \equiv |\psi|^2$, and at the tails $t \gg V^{-1}$ found strong deviations from the universal Porter-Thomas distribution [see Eqs. (6)–(8)] associated with the typically extended-type behavior. The universal statistics equally describe the quantum states of various classically chaotic systems; it depends on their fundamental symmetry, but not on the physical dimensionality or the level of disorder. Such a description can be successfully applied to most of the states (extended ones) in the metallic regime and gives the body of the distribution function of their local amplitudes. The deviations from the universal laws start rising at the amplitudes $t \sim \sqrt{g}/V$ and finally develop into completely different asymptotics at $t \sim g/V$. In dimensions $d = 2$ and 3, the form of the asymptotics is described by the logarithmically normal tails in Eqs. (10),(65),(73), whereas in Q1D wires it has a stronger dependence, $f \propto \exp\{-4\sqrt{\beta t L_c}\}$.

The scheme of calculus (see Secs. III and IV) and the similarity between our results for isolated systems and the asymptotics of distributions of the local density of states and fluctuations of other quantities in Q1D (Ref. 31) and 2D (Ref. 9) conductors indicate that the above-mentioned long tails are strongly influenced by the localization. To answer the question of how the localization develops, we can refer to the fact that the deviations from the Porter-Thomas distribution appear as a small number of events, $\propto \exp(-\sqrt{g})$, and that their occurrence near the Fermi level in a specific sample is a typically mesoscopic phenomenon. We interpret this as the rare top-amplitude splashes are not locally implicit as portions to any state, but represent very nontrivial configurations of waves, which can be found more and more often if the disorder increases. The analysis of the cross correlations $R(t,r)$ also indicates that the states, which are responsible for locally the highest amplitudes $|\psi(\mathbf{r}_0)|^2 > g/V$, have individually specific envelopes of their decaying density far away from the observation point $\mathbf{r}_0$. In Q1D and 2D systems, the tails of the envelopes obey the power-law dependence $|\psi(\mathbf{r}_0+\mathbf{r})|^2 \propto r^{-2\mu}$. In wires, $\mu = 1$, so that the density of these tails is perfectly integrable at long distances, and one could speak about them as nearly localized ones. In dimension $d = 2$, the exponent $\mu$ is limited by $\mu(t) \leq 1$ (so that it is not the localization in the usual sense) and is individual for the states with different amplitudes of the top splash. Such a behavior of prelocalized states in $d = 2$ coexists with the typically multifractal behavior of the inverse participation numbers, which has been observed earlier in various numerical simulations at critical conditions of the localization-delocalization transition.[10–15] Unfortunately, at the present stage we cannot approach close to the 3D Anderson transition and check the multifractality globally. Nevertheless, even in $d = 3$, we find the nontrivial logarithmically normal asymptotic behavior of the statistics, although the states, which seem to be responsible for that, are not localized.

The combination of the facts presented above forces us to suggest that the details of the structure and unusual statistics of rare prelocalized states, which we were discussing, have something to do with the statistics of extraordinary multiply self-crossing diffusive paths which anomalously often return to the same spatial coordinates $\mathbf{r}_0$. In some sense, the anomalous events are analogous to the scars in wave functions found by Heller[45,46] in chaotic ballistic cavities, although in disordered conductor they have a stochastic nature. Using the language of path integrals, the "prelocalized" states develop, because of rare shortened classical trajectories, which form a closed loop not only in the real space, but also in the full phase space, since they finally come to the same "cell" $dpdx = \hbar$ where they started. For instance, the most dense configuration could be formed by a forward-and-backward scattered trajectory of a particle bouncing few impurities. An additional argument, which supports this scenario, relates to the conditions limiting the validity of our theory. Based on the use of the $\sigma$ model, we have found it necessary to cut the linear length scale of the supermatrix $Q$-field variation from below, by the value of the mean free path. Nevertheless, the densities, which can be described in our approach, are limited by the value $1/(l\lambda_F^{d-1})$ instead of a naively expected inverse volume $l^{-d}$. This is only possible if the states that we study are

locally anisotropic at the fine scale of distances of about $l$ and typically have a snakelike structure with the cross-sectional width $\sim \lambda_F^{d-1}$.

## ACKNOWLEDGMENTS

We are grateful to B. Altshuler, M. Janssen, B. Kramer, I. Lerner, B. Simons, and M. Schreiber for useful discussions and thank P. Fulde for continuous encouragements during all the time we worked on this problem. We especially acknowledge discussions with V. Kravtsov and his comments on the manuscript which helped us to improve it. One of the authors (V.F.) acknowledges partial support from NATO Collaborative Research Grant No. 921333.

## APPENDIX A: PREEXPONENTIAL FACTOR FOR QUASI-ONE-DIMENSIONAL CASE

In this Appendix, we show some details of calculations of the preexponential factor $J$ for the Q1D case. Due to the condition $\theta_t = 0$ at $x = x_0$, the observation point splits the interval $[0, L]$ into two pieces, and the spectrum $\{\chi(n)\}$ of fluctuations around the saddle-point solution can be found in each interval separately. Therefore, we represent the preexponential as a product $J = J_L J_R$ of contributions from the left- and right-hand-side intervals with lengths $L_{L,R}$, where each of $J_{L,R}$ is determined by the eigenvalues of the Schrödinger equation in Eq. (48), with the symmetry-breaking potentials,

$$U_i = \left[ kT_i + \kappa \left( \left[ \frac{\sqrt{T_i}\pi/2}{1+\sqrt{T_i}} \right] \Big/ \sin\left\{ \frac{\sqrt{T_i}\pi/2}{1+\sqrt{T_i}} \frac{x}{L_i} \right\} \right)^2 \right] L_i^{-2} ,$$

where $i = L, R$. When $T \ll 1$ (in the paragraph below, we omit indices $L$ and $R$), these potentials can be treated perturbatively. Their first-order corrections cancel, due to the sum rule from Eq. (50), so that $J \approx 1 + T^2 \approx 1$. When $T \gg 1$, the same cancellation eliminates contributions from the high-excitation eigenvalues $\chi > (\pi/2L)^2 T$, so that the important contribution comes from the low-energy part of the spectrum, $\chi < (\pi/2L)^2 T$, where one can approximate

$$U \approx (\pi/2L)^2 [k + k'/\sin^2(\pi x/2L)], \quad k' = k + \kappa.$$

Using this approximation, the spectral problem of 1D Eq. (48) can be solved exactly. To find the exact solution, one has to change variables from $x$ to $y = \cot(\pi x/2L)$ and then seek solutions in the form $\phi = P_n(y^2)/(1+y^2)^{\delta(n)}$, where $P_n(y^2)$ are polynomials. This results in the set of eigenvalues $\chi(n)$, $n \geq 0$,

$$\chi(n) = (\pi/2L)^2 \left\{ \left[ 2n + 1/2 + \sqrt{k' + 1/4} \right]^2 - k \right\} .$$

Being substituted into Eq. (47), this gives the preexponential factor $J$ in the main order in $T_{L,R}$:

$$J \approx \exp\left( \sum_{i=L,R} \frac{1}{4} \ln T_i + \text{const} \right) \approx C\,(T_L T_R)^{1/4} . \quad \text{(A1)}$$

## APPENDIX B: PREEXPONENTIAL FACTOR FOR 2D CASE

In the 2D case, the spectrum $\{\chi(n,m)\}$ of fluctuations around the saddle point should be classified by orbital and radial quantum numbers $n$ and $m$, respectively, and can be found from the eigenvalues of the Hamiltonian,

$$\hat{H} = -r^{-1}\partial_r(r\partial_r) + m^2 r^{-2} + U ,$$

where $U$ is determined by Eq. (49).

Without any symmetry breaking, the spectrum of $\chi$'s can be approximated as

$$\chi(0,0) \approx 2L^{-2}/\ln(L/l) \quad \text{(B1)}$$

for the lowest mode and as

$$\chi(n,m) \approx \left(\frac{\pi}{L}\right)^2 \left[ n + \frac{1}{4} + \frac{m}{2} \right]^2 \quad \text{(B2)}$$

for higher $n$'s and $m$'s.

The optimal solution breaks the fermion-boson symmetry and induces effective potentials composed of two types of contributions,

$$\frac{1}{4}k(\partial\theta_t)^2 \approx k\mu^2/r^2 \text{ and } \quad \kappa \frac{t}{2\pi\nu D} e^{-\theta_t} \approx \kappa\mu L^{-2} \left(\frac{L}{r}\right)^{2\mu} .$$

In the above equations, the approximate values are given for the most important range of distances $r \leq L\sqrt{z(T)/T}$, and one has to remember that $\mu < 1$.

For any $m \neq 0$, the potential $U$ is relatively small, $U \ll m^2/r^2$, and could be treated perturbatively. Due to the sum rule mentioned in Sec. III D, Eq. (50), the modes with $m \neq 0$ contribute only in the second order in $U$, and what they give to the exponential of $J$ is of the order of $\mu^4 \ln(L/l); \mu^2$. With the accuracy we need here regarding the leading terms in $F_t$, this contribution can be neglected.

The spectrum of low-lying modes $\{\chi(n > 0, 0)\}$ is given by the expression

$$\chi(n,0) \sim \left(\frac{\pi}{L}\right)^2 \left[ n + \frac{1}{4} + \sqrt{k}\frac{\mu}{2} \right]^2 , \quad 0 < n \leq \frac{L}{\pi l} . \quad \text{(B3)}$$

The cancellation between different eigenvalues from Eqs. (B1)–(B3) substituted to the general equation in Eq. (47) produces a multiplier to $J$, which is of the order of $e^{\sim\mu^2}$ for $T \ll 1$ and $\mu \ln \frac{L}{l}$, at $T \gg 1$. Finally, we get

$$J = 1 + 0(T^2), \; T \ll 1 ,$$
$$J \propto \mu \exp\left(\mu \ln \frac{L}{l}\right) \sim T, \; T \gg 1.$$

This result can be used for all symmetry classes.

* Present address: Dept. of Theoretical Physics, University of Oxford, 1 Keble Road, OX1 3NP Oxford, United Kingdom.
[1] P.W. Anderson, Phys. Rev. **109B**, 1492 (1958).
[2] D. Thouless, Phys. Rev. Lett. **39**, 1792 (1972).
[3] M. Kaveh and N. Mott, J. Phys. C **15**, L697 (1982); **15**, L707 (1982).
[4] F. Wegner, Z. Phys. B **35**, 207 (1979).
[5] P.A. Lee and T.V. Ramakrishnan, Rev. Mod. Phys. **57**, 287 (1985), and references therein.
[6] B. Kramer and A. MacKinnon, Rep. Prog. Phys. **56**, 1469 (1993), and references therein.
[7] K.B. Efetov, Adv. Phys. **32**, 53 (1983).
[8] F. Wegner, Z. Phys. B **36**, 209 (1980).
[9] B.L. Altshuler, V.E. Kravtsov, and I.V. Lerner, in *Mesoscopic Phenomena in Solids*, edited by B.L. Altshuler *et al.* (Elsevier, Amsterdam, 1991), p. 449, and references therein.
[10] H. Aoki, J. Phys. C **16,** L205 (1983); Phys. Rev. B **33,** 7310 (1985).
[11] M. Schreiber, J. Phys. C **18,** 2493 (1985); Phys. Rev. B **31,** 6146 (1985); M. Schreiber and H. Grussbach, Phys. Rev. Lett. **67**, 607 (1991); H. Grussbach and M. Schreiber, Phys. Rev. B **48**, 6650 (1993); **51**, 663 (1995).
[12] B. Kramer, Y. Ono, and T. Ohtsuki, Surf. Sci. **196,** 127 (1988).
[13] T. Karawarabayashi and T. Ohtsuki, Phys. Rev. B **51**, 10 897 (1995).
[14] S. Evangelou and D. Katsanos, J. Phys. A **26**, L1243 (1993).
[15] M. Janssen, O. Viehweger, U. Fastenrath, and J. Hajdu, *Introduction to the Theory of the Integer Quantum Hall Effect* (VCH, Weinheim, 1994); W. Pook and M. Janssen, Z. Phys. B **82**, 295 (1991); U. Fastenrath, M. Janssen, and W. Pook, Physica A **191**, 401 (1992).
[16] C. Castellani and L. Peliti, J. Phys. A **19,** L429 (1986).
[17] B.A. Muzykantskii and D.E. Khmelnitskii, Phys. Rev. B **51**, 5480 (1995).
[18] L.P. Gorkov and G.M. Eliashberg, Zh. Eksp. Teor. Fiz. **48,** 1407 (1965) [Sov. Phys. JETP **21,** 940 (1965)].
[19] T.A. Brody, J. Flores, J.B. French, P.A. Mello, A. Pandey, and S.S.M. Wong, Rev. Mod. Phys. **53**, 385 (1981); J.J.M. Verbaarschot, H.A. Weidenmuller, and M.R. Zirnbauer, Phys. Rep. **129**, 367 (1985).
[20] M. Berry, Proc. R. Soc. London Ser. A **400**, 229 (1985).
[21] R.A. Jalabert, A.D. Stone, and Y. Alhassid, Phys. Rev. Lett. **68**, 3468 (1992).
[22] K.B. Efetov and V.N. Prigodin, Phys. Rev. Lett. **70**, 1315 (1993).
[23] B.D. Simons and B.L. Altshuler, Phys. Rev. Lett. **70**, 4063 (1993); Phys. Rev. B **48**, 5422 (1993).
[24] V.N. Prigodin, K.B. Efetov, and S. Iida, Phys. Rev. Lett. **71,** 1230 (1993).
[25] V.I. Fal'ko and K.B. Efetov, Phys. Rev. B **50**, 11 267 (1994).
[26] Y.V. Fyodorov and A.D. Mirlin, Pis'ma Zh. Eksp. Teor. Fiz. **60**, 779 (1994) [JETP Lett. **60**, 790 (1994)].
[27] "Intrinsic" conductance $g$ depends on the dimensionality of the system:

$$1\mathrm{D}: \; g \sim \frac{L_c}{L}; \quad 2\mathrm{D}: \; g \sim \frac{p_F l}{\ln(L/l)}; \quad 3\mathrm{D}: \; g \sim (p_F l)^2.$$

Here, we speak about the dimensionless conductance, $g \equiv G/(e^2/h)$.
[28] W. Feller, *Introduction to Probability Theory and Its Applications* (Wiley, New York, 1966).
[29] It is worth mentioning that $f(\downarrow, t)$ is normalized, $t_0 = 1$, and the normalization of spin-projected wave functions, $t_1 = 1/(2V)$, produces the same requirement as in Eq. (28).
[30] B.L. Altshuler and V.N. Prigodin, Zh. Eksp. Teor. Fiz. **95,** 348 (1989) [Sov. Phys. JETP **68,** 198 (1989)].
[31] A.D. Mirlin and Y.V. Fyodorov, J. Phys. A **26**, L551 (1993).
[32] A.D. Mirlin and Y.V. Fyodorov, Phys. Rev. Lett. **72**, 526 (1994).
[33] V.I. Fal'ko and K.B. Efetov, Europhys. Lett. (to be published).
[34] By this term, we denote the class of the systems both with the spin-dependent mechanism of scattering and broken time-reversal symmetry. For instance, this can be imagined as a metal with built-in disordered static magnetic field or a random exchange field.
[35] B. DeWitt, *Supermanifolds* (Cambridge University Press, Cambridge, 1992).
[36] C. Itzykson and J.-M. Drouffe, *Statistical Field Theory*, (Cambridge Press, Cambridge, England, 1989), Vol. 1.
[37] V.E. Kravtsov, I.V. Lerner, and V.I. Yudson, Phys. Lett. A **134**, 245 (1989).
[38] G. Castilla and S. Chakravarty, Phys. Rev. Lett. **71**, 384 (1993).
[39] F. Wegner, Z. Phys. B **78**, 33 (1990).
[40] K.B. Efetov and A.I. Larkin, Zh. Eksp. Teor. Fiz. **85,** 764 (1983) [Sov. Phys. JETP **58,** 444 (1983)].
[41] R. Feynman, Rev. Mod. Phys. **20**, 367 (1948).
[42] E. Kamke, *Differential Equations* (Chelsea, New York, 1971).
[43] K.B. Efetov, Zh. Eksp. Teor. Fiz. **92**, 638 (1987) [Sov. Phys. JETP **65**, 360 (1987)].
[44] A. Kudroli, V. Kidambi, and S. Sridhar, Phys. Rev. Lett. **75**, 822 (1995).
[45] E.J. Heller, Phys. Rev. Lett. **53**, 1515 (1984); Phys. Rev. A **35**, 1360 (1987); E.J. Heller, P.W. O'Connor, and J. Gehlen, Phys. Scr. **40**, 354 (1989).
[46] E.G. Bogomolnyi, Physica D **31**, 169 (1988); M.V. Berry, Proc. R. Soc. London Ser. A **423**, 219 (1989).